Microoxen: Microorganisms to move microscale loads

Douglas B. Weibel, Piotr Garstecki, Declan Ryan, Willow R. DiLuzio, Michael Mayer, Jennifer E. Seto, and George M. Whitesides*

Department of Chemistry and Chemical Biology, Harvard University, 12 Oxford Street, Cambridge, MA 02138

Contributed by George M. Whitesides, July 12, 2005

It is difficult to harness the power generated by biological motors to carry out mechanical work in systems outside the cell. Efforts to capture the mechanical energy of nanomotors *ex vivo* require *in vitro* reconstitution of motor proteins and, often, protein engineering. This study presents a method for harnessing the power produced by biological motors that uses intact cells. The unicellular, biflagellated algae *Chlamydomonas reinhardtii* serve as "microoxen." This method uses surface chemistry to attach loads (1- to 6-μm-diameter polystyrene beads) to cells, phototaxis to steer swimming cells, and photochemistry to release loads. These motile microorganisms can transport microscale loads (3-μm-diameter beads) at velocities of $\approx$100–200 μm·sec^{-1} and over distances as large as 20 cm.

biological motors | *Chlamydomonas* | phototaxis | microfluidics | microspheres

This study demonstrates the biological propulsion of microscale loads by the unicellular photosynthetic algae *Chlamydomonas reinhardtii* (*CR*). We exploit the chemistry of the algal cell wall to attach single 1- to 6-μm polymer beads to *CR*. Cells with these "loads" attached swim at velocities as high as 100–200 μm·sec^{-1}, approximately the velocity of unmodified cells. *CR* is phototactic and can be guided by using visible light ($\lambda \approx 500$ nm); we have used this phototaxis to control the transport of microscale loads. A photocleavable linker between the surface of the bead and the cell wall allows us to release loads from the surface of the cell photochemically. We have combined these processes to pick up, transport, guide, and drop off beads by using motile cells.

There are many examples of nanometer-scale motors in nature. Within the cell, linear motors, including DNA and RNA polymerase, dyneins, kinesins, and myosin, play a critical role in transcription, mitosis, meiosis, muscle contraction, and transporting organelles and synaptic vesicles (1–5). In eukaryotic mitochondria, a rotary motor, ATP synthase, produces ATP by harnessing the flow of protons down an electrochemical proton gradient (6, 7). Outside of the cell, ciliary dyneins drive the beating of eukaryotic flagella and cilia. In bacteria, a complex of $\approx$20 proteins makes up the remarkable rotary motor that powers the motion of flagella (8).

Interest in biological motors is based on both their transduction of energy and their small size and hence their possible relevance to micro/nanotechnology; the remarkable work of Walker, Vale, Kinosita, Hirokawa, Yanagida and others (9–17) has transformed our understanding of molecular motors. One outcome has been the design and fabrication of new synthetic motors composed entirely of biological molecules (18, 19); another outcome has been the integration of components onto recombinant biological motors (20–22).

Here, we use biological motors intact in cells that use flagella (23). An advantage of this strategy over that using isolated and reconstituted motors is its simplicity. It (*i*) avoids purification and reconstitution of individual motor proteins, (*ii*) takes advantage of ATP and ion gradients generated by the cells and allows sensors already present in the cell (or introduced through genetic engineering) to be used, and (*iii*) makes it practical to use complex organelles (e.g., cilia) and integrated motions. By using the intact organism to transport objects, taking advantage of appropriate stimuli to guide them, and using chemistry to attach and detach the loads, we have constructed what we consider a micrometer-scale analog of an ox: that is, a microscale beast of burden.

We chose the unicellular photosynthetic algae *CR* to transport microscale loads. This organism is easy to culture and relatively insensitive to the details of its environment. *CR* cells are approximately spherical in shape and 10 μm in diameter; they use two flagella ($\approx$12 μm long) for locomotion (24, 25). Eukaryotic flagella are linear motors containing an inner core of microtubules and associated motor proteins (the axoneme) surrounded by a flagellar membrane (26). The axoneme of *CR* is several hundred nanometers in diameter and, when beaten synchronously (in a motion reminiscent of the breaststroke in swimming) at a frequency of $\approx$40–60 Hz, is capable of generating enough power to propel a cell through water at a velocity of $\approx$100–200 μm·sec^{-1} (Fig. 1*A*) (25); swimming cells rotate counterclockwise around their longitudinal axis at a frequency of 2 Hz and trace out a helical path (25). Cells of *CR* display chemotactic, phototactic, geotactic, and gyrotactic behavior; in principle, all of these phenotypes can be used to guide the movement of cells (26). We used the phototropism of *CR* to control the direction in which motile cells transported loads.

The cell wall of *CR* is a multilayered structure composed primarily of 4-hydroxyproline (4-HP)-rich glycopeptides. This cell wall comprises a thin crystalline outer domain and an amorphous inner domain (27). The structure of the cell wall arises from a combination of covalent and noncovalent interactions between glycoproteins rich in 4-HP residues (26, 27). We hypothesized that synthetic 4-HP polypeptides might bind tightly to the cell wall by means of interactions similar to those found in the cell; polystyrene (PS) beads decorated with synthetic 4-HP polypeptides bound to the outer cell wall by means of interactions that we presume are noncovalent. Incorporation of a photocleavable group, 4-[4-(1-aminoethyl)-2-methoxy-5-nitrophenoxy]-butanoic acid (NPOP), into the peptide allowed detachment of loads from cells by irradiation with UV light (λ = 365 nm) (28).

Materials and Methods

Reagents. Modified PS microspheres (1- to 6-μm diameter) were purchased from Polysciences. We used noncrosslinked PS microspheres (ρ = 1.05 g·cm^{-3}) because they closely matched the density of *CR* (ρ = 1.05–1.07 g·cm^{-3}). Fluorenylmethoxycarbonyl (Fmoc)-protected amino acids and 4-[4-[1-[[(9H-fluoren-9-ylmethoxy)carbonyl]amino]ethyl]-2-methoxy-5-nitrophenoxy]-butanoic acid were purchased from Advanced ChemTech. Peptides were synthesized on a MilliGen 9050 peptide synthesizer using standard Fmoc/2-(1H-benzotriazole-1-yl)1,1,3,3-

Abbreviations: *CR*, *Chlamydomonas reinhardtii*; 4-HP, 4-hydroxyproline; PS, polystyrene; NPOP, 4-[4-(1-aminoethyl)-2-methoxy-5-nitrophenoxy]-butanoic acid; NHS, *N*-hydroxysuccinimide; EDC, *N*-(3-dimethylaminopropyl)-*N*′-ethylcarbodiimide; PDMS, poly(dimethylsiloxane).

*To whom correspondence should be addressed. E-mail: gwhitesides@gmwgroup.harvard.edu.

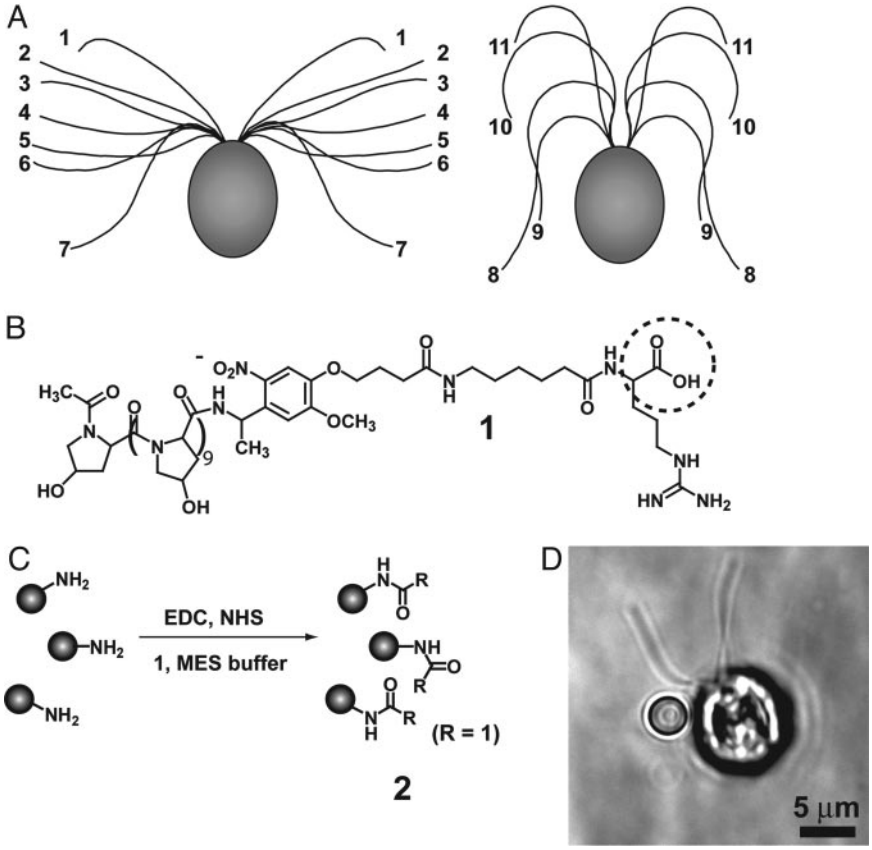

Fig. 1. An approach for attaching microscale loads to cells of *CR*. (*A*) A cartoon depicting the movement of the flagella of *CR* during a beat sequence. The starting position is labeled 1. The numbers indicate the position of the flagella during a single beat; a beat contains two components: the power stroke (positions 1–7) and the recovery stroke (positions 8–11). This cartoon is adapted from ref. 26. (*B*) The structure of peptide **1** used to attach beads to cells of *CR*. (*C*) The reaction used to derivatize amine-modified PS beads (3-μm diameter) with peptide **1** using NHS and EDC in Mes buffer (pH 5.4); the carboxylic acid that is activated and forms an amide bond is circled. The resulting beads, **2**, attached to the cell wall of *CR*. To simplify the scheme, only one amine group is shown per bead (**1**); the number of amine groups per bead is $\approx 2 \times 10^8$. (*D*) An image of bead **2** attached to a cell of *CR* acquired by using bright-field microscopy; the bead is attached to the top of the cell and appears slightly out of focus. (Magnification: $\times$100.)

tetramethyluronium tetrafluoroborate/hydroxybenzotriazole coupling chemistry (29). *N*-hydroxysuccinimide (NHS) and *N*-(3-dimethylaminopropyl)-*N*′-ethylcarbodiimide (EDC) were purchased from Alfa Aesar (Ward Hill, MA); Mes [2-(*N*-morpholino)ethanesulfonic acid] buffer was purchased from Hampton Research (Aliso Viejo, CA). Wild-type *CR* Dangeard was purchased from American Type Culture Collection (www.atcc.org) (no. 18798). We used Millipore MilliQ water for all experiments with cells and in all media. Poly(dimethylsiloxane) (PDMS) (Sylgard 184) was purchased from Essex Brownell (Chicago). Blue/green LEDs were purchased from LED Light (Carson City, NV). SU-8 50 and SU-8 100 were purchased from Microchem (Newton, MA). Silicon wafers were purchased from Silicon Sense (Nashua, NH).

Cell Culture. Synchronous cultures of *CR* were grown in American Type Culture Collection sporulation medium no. 5 (0.03% yeast extract/0.03% beef extract/0.06% tryptose/0.3% glucose, pH 7.2) using a 14/10-hr light/dark cycle. The culture was illuminated with a series of fluorescent grow lights. We found that bubbling CO_2 into the medium had a negligible effect on the growth rate of the culture. Cultures were typically grown to midlogarithm phase (a density of $\approx 10^5$ cells·ml^{-1}) before cells were harvested for experiments. We concentrated these cultures to $\approx 10^7$ cells·ml^{-1} by centrifugation for 5 min at 700 $\times$ *g*.

Fabrication of Microfluidic Networks. We fabricated microfluidic channels by using established procedures for rapid prototyping (30, 31). Briefly, we used photolithography to fabricate features in SU-8 photoresist (SU-8 2050 or SU-8 2100) on silicon wafers; masters were silanized by using a vapor of (tridecafluoro-1,1,2,2-tetrahydrooctyl)trichlorosilane. PDMS was poured on the master and cured thermally (70°C); the resulting layer of PDMS contained the microfluidic channels. Glass slides coated with PDMS were prepared by spin-coating thin layers of PDMS ($\approx$150-μm thick); the slides were cured thermally (70°C). Channels were fabricated by oxidizing both PDMS-coated slides and layers of PDMS containing channels in an oxygen plasma and sealed by pressing the surfaces into contact. Microfluidic channels were immediately filled with a solution of water; the water was exchanged for 5% BSA (in PBS buffer) and incubated for 8 hr at 4°C.

Passivating Microfluidic Channels. Cells rapidly adsorbed on different types of glass, polycarbonate, and surfaces coated with long polyethylene glycols; the adsorption of cells on PS was slower but still led to >80% of the cells on the surface after $\approx$1 hr. Passivating surfaces with BSA before adding cells improved the problem of cell adsorption moderately, as did adding 0.1% BSA to the cell media, but cells still deposited slowly onto glass or plastic surfaces. Oxidized PDMS provided an excellent surface for resisting the adsorption of cells. When we pretreated hydrophilic PDMS surfaces with BSA, we observed few cells adsorbing to the surface over a period of 10 hr (<5%).

Synthesis of 4-HP-Modified Beads. A 1.0-ml suspension of amino-modified PS beads (3-μm diameter, coefficient of variance = 5%, 1.68×10^9 beads·ml^{-1}) in an Eppendorf tube was centrifuged, and the supernatant was discarded. The beads were resuspended in 0.1 M Mes buffer (1 ml, pH 5.4) and concentrated by centrifugation; this step was repeated three times. The beads were resuspended in 0.1 M Mes buffer (1 ml, pH 4.5) containing 4-HP peptide **1** (5 mM), NHS (15 mM), and EDC (15 mM) (32). The tube was placed on a vortex shaker, gently agitated for 8 hr at 25°C, rinsed with 10 aliquots of Mes buffer (1 ml), and finally suspended in PBS (pH 7.2). We sonicated the suspension of beads briefly before using them in experiments.

Phototactic Propulsion Experiments. LEDs (500-nm wavelength) were integrated into the PDMS at both ends of microfluidic channels. Cells were concentrated by centrifugation for 5 min at $700 \times g$. The supernatant was removed, and cells were suspended in fresh American Type Culture Collection no. 5 medium. A 0.05% solution of functionalized PS beads in MilliQ water was premixed with a concentrated solution of cells and injected into microfluidic channels. The movement of beads by cells was observed by phase contrast microscopy. The direction in which beads were moved was controlled by applying a current of 0.2 A at 4.5 V to a single LED to induce negative phototaxis. By turning one LED off and the other on, cells could be induced to turn around and swim in the other lateral direction. Illuminating the LEDs out of phase caused cells to traverse back and forth within the channel; the same behavior was also observed with a single LED switched between a high and low intensity to induce negative and positive phototaxis, respectively. In channels $<$50-μm tall, cells deviated from a straight path during swimming, which may have arisen from contact between the flagella or cell body and the surfaces of the channel. Cells in channels 100-μm wide by 100-μm tall swam in smooth, straight paths during phototaxis.

Photocleavage of Beads from Cells. We carried out photocleavage experiments in microfluidic channels by using an 80-W mercury lamp as the light source, appropriate filters to pass only light with $\lambda = 365$ nm, and a $\times$20 objective to focus light. The amount of time required to release beads varied. To test the viability of cells exposed to UV light ($\lambda = 365$ nm), we exposed 50-ml liquid cultures of cells (density $\approx 10^2$ cells·ml^{-1}) to a high-power mercury lamp (100 W, $\approx$7 mW·cm^{-2} at 15 inches). The tubes were positioned 5 inches away from the surface of the bulb and were exposed for 5–15 min; the experiment was carried out in a laminar flow hood, where the circulation of air between the bulb and the tube prevented the tubes from heating significantly. All of the cultures exposed to UV light grew into liquid cultures with densities (10^5 cells·ml^{-1}) similar to those grown without UV exposure.

Results and Discussion

First, we developed a method of attaching PS beads to the cell wall of *CR*. PS beads displaying amine groups were functionalized with AcN(4-HP)$_{10}$-NPOP-Ax-Arg peptides (**1**, 4-HPP-NPOP) by means of its carboxyl group by using NHS and EDC in Mes buffer (pH 5.4) (Fig. 1 *B* and *C*) (32). The resulting beads bound to cells; amine-functionalized PS beads did not (Fig. 1*D*) (see *Supporting Text*, which is published as supporting information on the PNAS web site). A suspension of *CR* (10^7 cells, 1 ml) incubated with a suspension of 4-HPP-NPOP-coated beads (6×10^6 beads, 25 μl) led to beads attached to $\approx$80% of the cells; the number of beads per cell could be controlled by adjusting the relative concentration of beads and cells and is probably influenced by steric effects.

Beads could also be attached to cells by guiding cells through microfluidic channels using phototaxis into a "pile" of beads; only a single collision was required to attach a bead to a cell. Remarkably, cells modified with beads frequently traveled at velocities approaching those of unmodified cells ($\approx$100–200 μm·sec^{-1}). The position of the bead on the cell influenced the velocity with which it swam: Beads attached on or close to the flagella typically impeded swimming; beads located farther away did not. Although the majority of motile cells carried one or two beads, occasionally, cells transported larger numbers of beads. We observed cells with as many as 5 or more 3-μm-diameter beads traveling at a velocity of $>$100 μm·sec^{-1}; beads covered with $>$10 beads were still motile.

The location of beads attached to the cell appeared to be random. Beads attached to the posterior (the side of the cell opposite the flagella), the side, the flagella, or the anterior of the

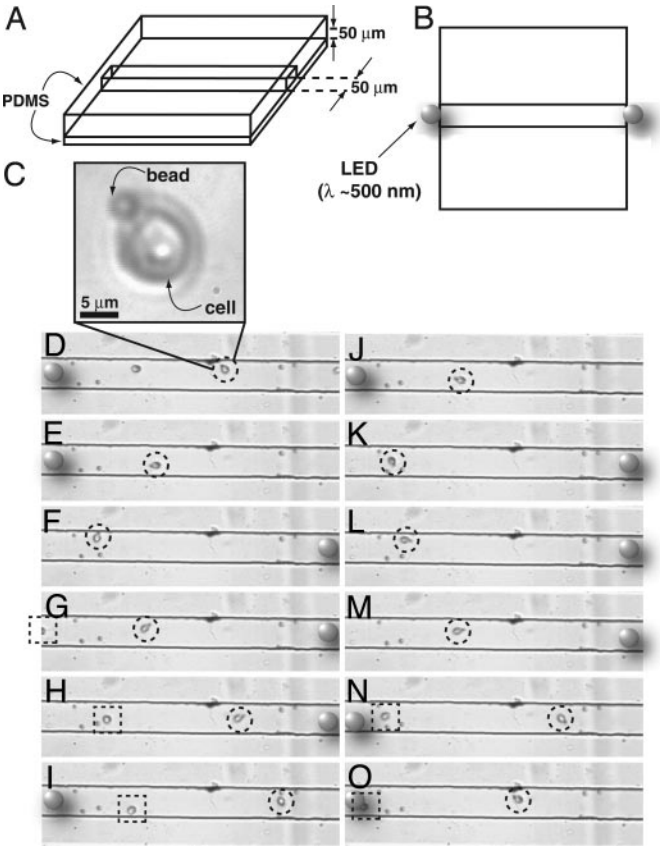

Fig. 2. Cells of *CR* with microscale loads attached are steered by using phototaxis. (*A*) A schematic (side view) of the microfluidic channels used in experiments to steer cells of *CR* with loads phototactically. The microfluidic device contained 25 parallel channels; for clarity, only one channel is shown. (*B*) Top view of the channels, including a cartoon depicting the position of the LEDs. (*C*) An image of a cell of *CR* with a PS bead attached (3-μm diameter) swimming in a channel; the cell was imaged by using phase contrast microscopy. The bead is attached to the cell wall between the two flagella. (Magnification: $\times$60.) (*D–O*) A sequence of images showing how the cell in *C* can be "steered" by using positive phototaxis; a dashed circle has been added to each frame to indicate the position of the cell. The LEDs embedded at both ends of the channel were illuminated alternately; in response, the cell swam back and forth within a region of the microfluidic channel. In the images, an illuminated LED is suggested by the presence of a cartoon of the LED. The cell made sharp, 180° turns when the direction of the gradient of light was changed by switching between the two LEDs. Images were acquired by using phase contrast microscopy. The time elapsed between images is 0.5 sec. The position of the stage remained stationary. To gauge how the velocity of the cell carrying a load differed from a cell without a bead, we introduced a second cell into the channel; this cell is indicated by the dashed square in *G–I*, *N*, and *O*. (Magnification: $\times$40.)

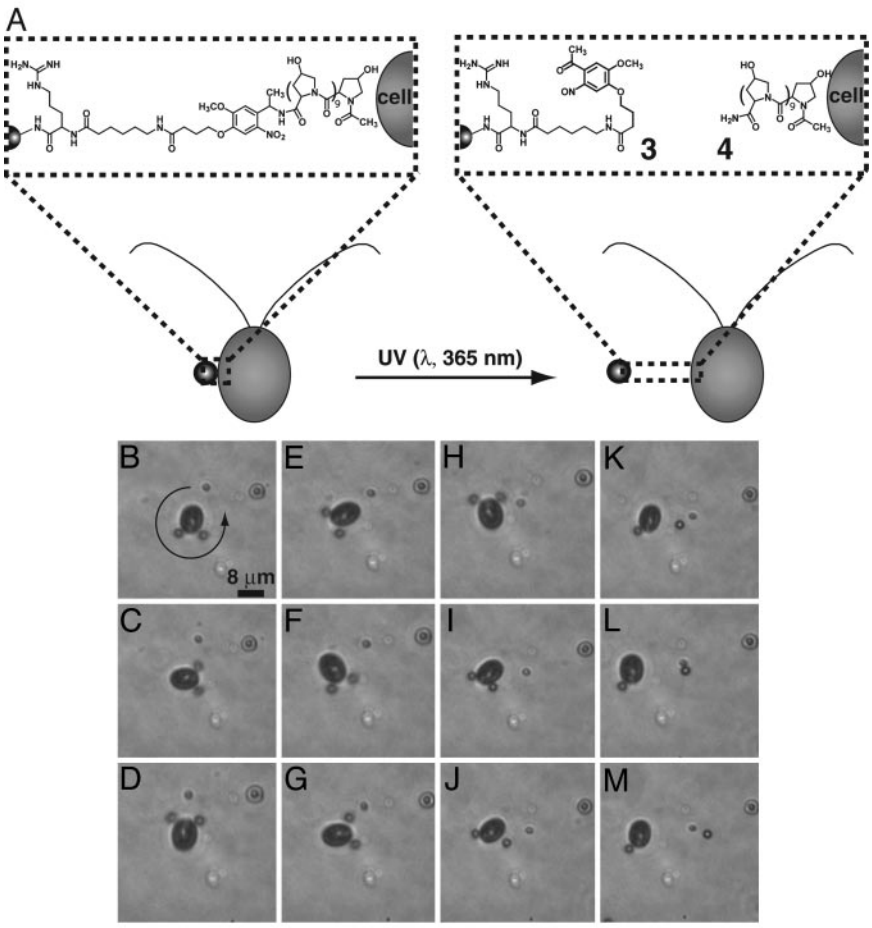

Fig. 3. Photochemical release of beads from cells of *CR* in microfluidic systems. (*A*) A cartoon depicting the photochemical cleavage of the beads from cells; the two fragments are a methyl ketone (**3**) and a primary amide (**4**). (*B–M*) A series of chronological images showing the photochemical release of a bead from a cell with two PS beads (3-μm diameter) attached. The cell was illuminated with UV light (λ = 365 nm, 80 W) for 20 sec before the image in frame 1 was acquired. The arrow in frame 1 indicates the direction in which the cell is rotating. The time that had elapsed between the frames was 2 sec. After 18 sec (*J*), the bead was released from the cell and slowly diffused away. We presume that this interval reflects the time for the initial photoproduct to cleave. The cell was imaged by using phase contrast microscopy. (Magnification: ×40.)

cell and adjacent to or between the two flagella. Surprisingly, cells with a bead bound directly between the flagella swam at a velocity of >100 μm·sec^{-1}. Beads remained attached to swimming cells and did not dislodge when the bead was bumped into the walls of the channel or another cell. HPP-NPOP-coated PS beads containing superparamagnetic cores provided another tool for manipulating *CR*. An external magnet could be used to drag cells attached to these beads through the medium at velocities of <250 μm·sec^{-1}; beads could not be separated from cells. We assume that the strong interaction between beads and cells is a product of many noncovalent interactions.

Cells frequently stuck irreversibly to the surface of glass and polymers; this sticking made it difficult to track motile *CR* cells carrying objects for significant periods of time. To prevent adhesion of *CR* to the surface of the microfluidic systems we used to investigate them, we used microsystems that were fabricated in PDMS and then oxidized and treated with BSA (33). This combination of surface and surfactant made it possible to study the movement of cells in microfluidic channels for ≈8 hr without significant adhesion (<5%) of cells on the surface of channels (see *Materials and Methods*).

Phototaxis provided a way to steer *CR* carrying loads in microfluidic systems. The action spectrum for phototaxis in *CR* is bimodal, with a maximum response at 505 nm and a secondary peak at 443 nm (25). At a high intensity of light, cells display negative phototaxis, swimming away from the light source, whereas at a lower intensity, cells display positive phototaxis and swim toward the light source; *CR* is phototactic over a range of intensity from 10^{11} to 10^{15} quanta·cm^{-2}·sec^{-1} at λ = 500 nm (25). The cells swam in microfluidic channels (50 μm wide × 50 μm tall) with LEDs imbedded in the PDMS at both ends of the channels to investigate the phototactic behavior of *CR* (Fig. 2*A*); the LEDs had a diameter of 5 mm, an emission maximum centered at λ = 505 nm, and a cutoff for emission at λ = 450 and 575 nm. Cells had a rapid phototactic response (<1 sec) and could be switched among random swimming, positive, and negative modes of phototaxis by varying the intensity of the LEDs; the response time for *CR* is reported to be ≈20 msec (25). In microfluidic channels that were 2–3 cm long, the intensity of the LED could be set so that phototaxis (both positive and negative) persisted over the entire length of the channel without readjusting the LED. Cells carrying loads also responded to gradients of light; when the LEDs at each end of a microfluidic channel were turned on and off, cells carrying PS beads (3-μm diameter) swam back and forth repeatedly along channels for 2–3 hr (Fig. 2*B*; see also Movie 1, which is published as supporting information on the PNAS web site). It should be possible, although it has been untested experimentally, to inte-

grate fiberoptics into microfluidic chambers to steer cells; this approach may produce more focused point sources of light than LEDs.

To test the endurance of cells transporting loads, we measured the distance that cells carried single PS beads (3-μm diameter) by guiding cells up and down the length of a 4-cm-long microfluidic channel by using negative phototaxis. Cells with beads attached routinely traversed distances of 16–20 cm at an average velocity of $\approx$100 μm·sec^{-1} before adhering to other cells, beads, or debris in the channels.

At a low Reynolds number, the viscous drag scales linearly with the velocity and radius of the moving object. A cell swimming at a velocity of 100 μm·sec^{-1} experiences a drag of $\approx$9 pN. The viscous drag on a 3-μm-diameter PS bead traveling at 100 μm·sec^{-1} is 2.8 pN. A bead attached to a cell modifies (increases) its drag by less than the drag of an individual sphere; the additional viscous drag introduced by the attached bead increases the overall drag of a cell by only a fraction of that on a free cell. Experiments confirm this analysis: Cells of *CR* carrying multiple PS beads (3-μm diameter) swim at a rate that approaches that of unmodified cells (100–200 μm·sec^{-1}).

UV irradiation of cells transporting beads released the loads (Fig. 3*A*). The beads we used (**2**) contained a spacer, NPOP, between the bead and the 4-HP sequence; the NPOP group cleaves upon exposure to light with λ = 365 nm (80 W, 60 sec) (28) (Fig. 1) and releases the bead (Fig. 3*B*; see also Movie 2, which is published as supporting information on the PNAS web site). After removing beads by photocleavage, cells swam away and could still be guided by phototaxis; cells exposed to UV light still replicated and could be used to seed new liquid cultures. Using a photochemical procedure to drop the load from the cell is particularly useful, because the area of a channel photoirradiated can be small, leaving other beads in the channel free to be picked up by cells. In principle, this method should be capable of guiding a cell to pick up and drop off individual loads repeatedly.

We have demonstrated a method of using the power generated by biological motors to transport loads while leaving these motors in intact cells. This approach has several attractive features: (*i*) no genetic engineering or protein purification is required, (*ii*) motors do not have to be reconstituted *in vitro*; they are already intact, (*iii*) using the whole cells provides a surface (the cell wall) on which objects can be attached, (*iv*) phenotypes can be exploited to "steer" the movement of swimming cells, (*v*) the cell provides the power, (*vi*) the entire system is easily replicated, simply by growing the organism (*CR* can be easily grown to a density of $\approx 10^7$ cells per liter), (*vii*) the procedure is not limited to PS beads, and the attachment does not require manipulating the motor itself, and (*viii*) the "fuel" for the motor is generated by the cell. A whole-cell approach does have the limitation that it is not applicable if the overall system (motor and load) must be nanoscale in size. We believe that using biological nanomotors intact in living cells may be a more practical strategy for their exploitation in many applications in biotechnology than separating them from the cell and using them in isolation.

This research was supported by grants from the Department of Energy (DE-FG02-OOER45852) and the National Institutes of Health (NIH) (GM065364). We used the Materials Research Science and Engineering Centers shared facilities supported by the National Science Foundation (NSF) under award no. DMR-0213805. This work was also supported by postdoctoral fellowships from the NIH (GM067445) (to D.B.W.), the Foundation for Polish Science (to P.G.), and the Swiss NSF (to M.M.); NSF-Integrative Graduate Education and Research Traineeship Biomechanics Training Grant DGE-0221682 (to W.R.D.); and the NSF Research Experiences for Undergraduates program (J.E.S.).

1. Yin, H., Wang, M. D., Svoboda, K., Landick, R., Block, S. M. & Gelles, J. (1995) *Science* **270,** 1653–1657.
2. Svoboda, K., Schmidt, C. F., Schnapp, B. J. & Block, S. M. (1993) *Nature* **365,** 721–727.
3. Vallee, R. B. & Hook, P. (2003) *Nature* **421,** 701–702.
4. Mermall, V., Post, P. L. & Mooseker, M. S. (1998) *Science* **279,** 527–533.
5. De La Cruz, E. M. & Ostap, E. M. (2004) *Curr. Opin. Cell Biol.* **16,** 61–67.
6. Stock, D., Leslie, A. G. W. & Walker, J. E. (1999) *Science* **286,** 1700–1705.
7. Boyer, P. D. (1993) *Biochim. Biophys. Acta* **1140,** 215–250.
8. Berg, H. C. (2003) *Annu. Rev. Biochem.* **72,** 19–54.
9. Gibbons, C., Montgomery, M. G., Leslie, A. G. W. & Walker, J. E. (2000) *Nat. Struct. Biol.* **7,** 1055–1061.
10. Nishizaka, T., Oiwa, K., Noji, H., Kimura, S., Muneyuki, E., Yoshida, M. & Kinosita, K. (2004) *Nat. Struct. Mol. Biol.* **11,** 142–148.
11. Hirokawa, N. (1998) *Science* **279,** 519–526.
12. Funatsu, T., Harada, Y., Tokunaga, M., Saito, K. & Yanagida, T. (1995) *Nature* **374,** 555–559.
13. Vale, R. D., Funatsu, T., Pierce, D. W., Romber, L. Harada, Y. & Yanagida, T. (1996) *Nature* **380,** 451–453.
14. Rondelez, Y., Tresset, G., Nakashima, T., Kato-Yamada, Y., Fujita, H., Takeuchi, S. & Noji, H. (2005) *Nature* **433,** 773–777.
15. Takahashi, Y., Edamatsu, M. & Toyoshima, Y. Y. (2004) *Proc. Natl. Acad. Sci. USA* **101,** 12865–12869.
16. Inoue, Y., Toyoshima, Y. Y., Iwane, A. H., Morimoto, S., Higuchi, H. & Yanagida, T. (1997) *Proc. Natl. Acad. Sci. USA* **94,** 7275–7280.
17. Yildiz, A., Tomishige, M., Vale, R. D. & Selvin, P. R. (2004) *Science* **303,** 676–679.
18. Mao, C., Sun, W., Shen, Z. & Seeman, N. C. (1999) *Nature* **397,** 144–146.
19. Chen, Y., Wang, M. & Mao, C. (2004) *Angew. Chem. Int. Ed.* **43,** 3554–3557.
20. Brunner, C., Karl-Heinz, E., Hess, H. & Vogel, V. (2004) *Nanotechnology* **15,** S540–S548.
21. Itoh, H., Takahashi, A., Adachi, K., Noji, H., Yasuda, R., Yoshida, M. & Kinosita, K. (2004) *Nature* **427,** 465–468.
22. Soong, R. K., Bachand, G. D., Neves, H. P., Olkhovets, A. G. & Montemagno, C. D. (2000) *Science* **290,** 1555–1558.
23. Darnton, N., Turner, L., Breuer, K. & Berg, H. (2004) *Biophys. J.* **86,** 1863–1870.
24. Silflow, C. D. & Lefebvre, P. A. (2001) *Plant Physiol.* **127,** 1500–1507.
25. Foster, K. W. & Smyth, R. D. *Microbiol. Rev.* **44**, 572–630.
26. Harris, H. E. (1989) *The Chlamydomonas Sourcebook* (Academic, San Diego), pp. 67–216.
27. Miller, D. H., Lamport, D. T. A. & Miller, M. (1972) *Science* **176,** 918–920.
28. Holmes, C. P. & Jones, D. G. (1995) *J. Org. Chem.* **60,** 2318–2319.
29. Fields, G. B. Lauer-Fields, J. L., Liu, R.-Q. & Barany, G. (2002) in *Synthetic Peptides: A User's Guide*, ed. Grant, G. A. (Oxford Univ. Press, New York), pp. 93–219.
30. Duffy, D. C., McDonald, J. C., Schueller, O. J. A. & Whitesides, G. M. (1998) *Anal. Chem.* **70,** 4974–4984.
31. Xia, Y. & Whitesides, G. M. (1998) *Angew. Chem. Int. Ed.* **37,** 550–575.
32. Bailey, P. D., Mills, T. J., Pettecrew, R. & Price, R. A. (2005) in *Comprehensive Organic Functional Group Transformations II*, eds. Katritzky, R. A. & Taylor, R. J. K. (Elsevier, London), pp. 201–294.
33. Whitesides, G. M., Ostuni, E., Takayama, S., Jiang, X. & Ingber, D. E. (2001) *Annu. Rev. Biomed. Eng.* **3,** 335–373.